Heliyon 9 (2023) e17431

Contents lists available at ScienceDirect

Heliyon

journal homepage: www.cell.com/heliyon

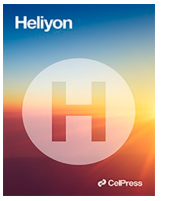

Synergistic effects of atomic oxygen and thermal cycling in low earth orbit on polymer-matrixed space material

Ruiqiong Zhai [a,*], Xiaoning Yang [a], Lixiang Jiang [a], Hong Gao [b], Yuxin Zhang [c], Zilong Jiao [a]

[a] Beijing Institute of Spacecraft Environment Engineering, Beijing, 100094, China
[b] China Aerospace Components Engineering Center, Beijing, China
[c] College of Materials Science and Engineering, Chongqing University, Chongqing, China

ARTICLE INFO

Keywords:
Polymer
Atomic oxygen (AO)
Thermal cycling (TC)
Synergistic effect
LEO environment

ABSTRACT

Polymer-matrixed materials are widely used in the spacecrafts' structures. However, crafts located in the LEO (Low Earth Orbit) would suffer from hazardous environment factors when orbiting in the space. It has been reported that the space environment factors' integral effect (which represents the factual detriment in space) is not equivalent to the simple summation of each individual. Hence, atomic oxygen and thermal cycling were selected as the starting point for studying the typical LEO synergistic effects on polymer-matrixed space material. In this work, methods such as surface morphology observation, surface components analyzation and inter-laminar-shear strength test were embraced to gather the basic information for the study of degradation. As a result, focusing on the composites selected in this work, synergistic effects do exist between the two factors (AO&TC, representing for atomic oxygen and thermal cycling combined). Besides, a quantified index was proposed to represent synergistic characteristics , so as to lay the foundation for the scientific evolution of material characterization.

1. Introduction

The carbon-fiber-reinforced polymers possess many advantages for Low Earth Orbit (LEO) spacecraft applications due to their superior properties, such as low mass, easy-processing, excellent thermo-optical properties and strength-to-mass ratio. However, when they are exposed into the space environment such as ultrahigh vacuum (UHV), atomic oxygen, charged particles, thermal cycling, ultraviolet radiation, orbital debris impacts [1–3], the polymers would definitely undergo severe degradation without appropriate protection [4–8].

Atomic oxygen (AO), which generates from UV-induced($E > 5.12eV$, $\lambda < 243nm$) dissociation of molecular oxygen, is a constituent of a particular concern for materials in the LEO environment [9,10]. Besides, it is regarded as the most severe hazard for spacecraft's external surfaces, due to its oxidative and erosive behavior [11–13]. It could lead to changes in optical deterioration [14] and mass loss [15] caused by cratering, internal and back-surface spallation [16], along with particulate and molecular contamination, and furtherly, induce the degradation in mechanical properties [17–20].

Worth to be noticed that, - in most cases, tests for effects of space environment factors could only be performed individually in the ground-based facilities; however, space materials are actually surviving in the space environment factors simultaneously in reality. It

* Corresponding author.
E-mail address: lingid_83@163.com (R. Zhai).

https://doi.org/10.1016/j.heliyon.2023.e17431
Received 9 May 2022; Received in revised form 15 June 2023; Accepted 16 June 2023
Available online 5 July 2023

indicates that, the ground-based tests may not be representative for reproducing the reactions taking place in the actual space exposure. So, it raises the interests of the researches to decide whether the integral space environment effect equals to the simple summation of each. -Based on some previous works delivered in the references, some of materials tell that the answers are not that direct and simple [21–28].

According to the previous results, under the other space factors such as UV, some material reveals harsher AO erosion in structure modification and surface roughening, leading to irreversible degradation of optical, thermal, electrical and mechanical properties [10]. However, there seems to be a vacancy focusing on AO interaction accompanied with thermal cycling (TC), where researchers seldom stepped in—once, AO and thermal exposure behavior had been studied [29,30], however the effects were tested and analyzed respectively; or, more efforts are needed to enrich or verify the results and unravel the mechanisms [31].

In late publication, some ceramic coatings are evaluated by measuring the thermal expansion coefficient and AO erosion rate [32], with a phenomenological modeling introduced to approach the relationship between erosion mechanism due to AO impact and surface energy variation induced by thermal cycles; such analysis highlights the importance of considering the synergistic effects between different aging factors(such as AO and TC), so as to achieve a reliable interpretation of the space environment's effect on spacecraft structures and materials.

That is part of the reason why the work in this paper was undertaken.

2. Research strategy

* CF/EP: carbon-fiber-reinforced epoxy; *CF/CE: carbon-fiber-reinforced cyanate ester
* LDEF: Long Duration Exposure Facility; *STS: Space Transportation System

Long-duration spacecrafts such as the ISS are generally located in the Low Earth Orbit, typically, at the altitude around 400 km. Among which, *atomic oxygen (AO)* and *thermal cycling (TC)* are the most typical space environment factors. Therefore, those two factors were selected to serve as a primary step to explore the space environment synergistic effects on the space material.

Unlike in the GEO environment, it is less probable for the spacecrafts to encounter with environment such as radiation or charged particles in most cases; besides, AO itself is electroneutral–therefore , only macro-indicator such as mechanical performance, along with optical observation and mass loss, was taken into consideration at the current stage, to set as the index to characterize the synergistic effects.

Given that the discussion was under the aspect of mechanical performance, two materials which are either prevalent used or with a great prospect of future usage, were selected as the test carrier for the study. The scheme of thoughts was demonstrated in Fig. 1.

3. Test method

3.1. Test materials

Carbon-fiber-reinforced epoxy(CF/EP) materials has already been utilized prevalently in the astronautic engineering, meanwhile, modified carbon-fiber-reinforced cyanate(CF/CE) materials has become a new tendency in space material selection nowadays.

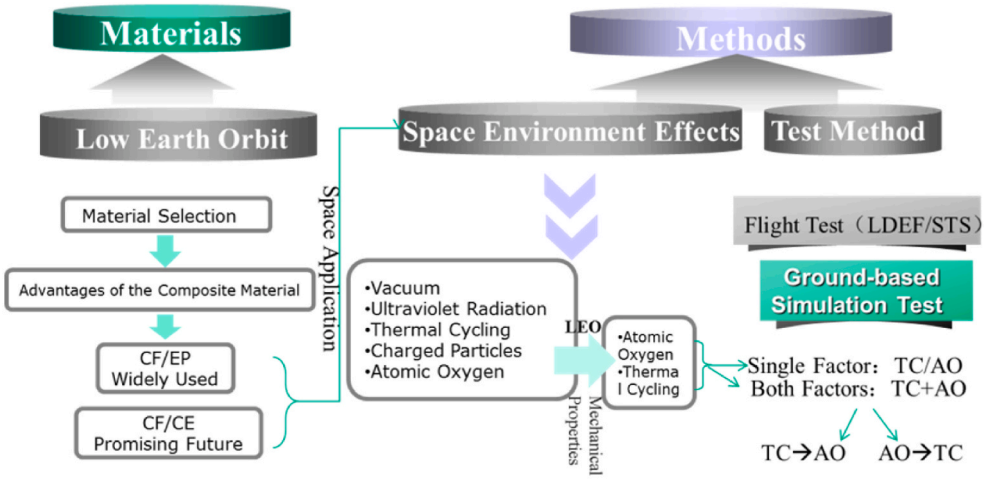

*CF/EP: carbon-fiber-reinforced epoxy; *CF/CE: carbon-fiber-reinforced cyanate ester

*LDEF: Long Duration Exposure Facility; *STS: Space Transportation System

Fig. 1. Research thoughts and structure.

Thus, two types of composite materials named M40/AG-80 (carbon-fiber-reinforced epoxy) and M40/DFA-1(carbon-fiber-reinforced cyanate) are selected as the test specimen in this study.

Each type of the material was divided into 5 groups labelled as ①/②/③/④/⑤ Group.

3.2. Test schedule

AO was nominated to refer to *Atomic Oxygen*, and TC was nominated to refer to *Thermal Cycling*. Group① was set to be stay original，while Group② was set to undergo AO test, Group③ to undergo TC test, Group④ to undergo (AO + TC) sequent test, Group⑤ to undergo (TC + AO) sequent test. Thus, as it shows in Fig. 2, only twice AO tests under the same condition and once TC test could be enough. —which means, at the first step, Group②+Group④ would join the first AO test; after that, Group③+Group④+Group⑤ were taken into the TC test; and at the last step, Group⑤ after TC test finished its second AO test. Till then, each group would accomplish its own "*Brand-Burning*"(represent its corresponding space environment factors), as it listed in Table S1 in the Appendix.

The test conditions are stated in section 3.3.1.

3.3. Test facilities and methods

3.3.1. Space environment test method

AO test was conducted in the AO impact facility at Beijing Institute of Spacecraft Environment Engineering(BISEE), as illustrated in Fig. 3, with sample positioning presented(Kapton K_m was laid in the middle, while Kapton K_e laid at the edge, so as to measure the actual AO fluence during test). The sample panel would be clamped inside the chamber, placed at the normal incidence facing towards the AO source.

Of which, the primary indexes are:

1) Vacuum degree：5×10^{-2}Pa
2) Area of Impact Flux：(diameter of the area) > 150cm3)Energy of the Flux：3 ~ 10eV
4) AO Flux:1.0×10^{16} atom/cm^2/s
5) AO fluence：1.5×1020 atom/cm2

TC test was conducted in the F-10(B) cryogenic test chamber at BISEE, of which, the primary indexes are:

1) Temperature range：-150 ~ 180 °C;
2) Heating Rate：>30 °C/min;

To avoid TC induced microcracks, test temperature was set to be in the range of [−150,+150]°C with 200 cycles, referring to reference [33–35].

3.3.2. Specimen performance test method

Thermo-oxidation process is intrinsically linked with the action mechanism and behavior of polymers [36]. Hence, multiple test methods are introduced into the performance evaluation. Mass loss test was conducted on the Miro Sartorius Precision Electronic Balance, with accuracy at 10^{-6} g. The specimens are weighed before and after space environment test, three times of each, recorded with average value; then, AO interaction rate could be deduced following "Kapton equivalent fluence" method as an ASTM standard of measurement [37], as it listed in Table 2 and Table 3. ，—following Equation (1) as below:

$$R_e = \frac{\Delta m/\rho}{f_k t \bullet A} = \frac{\Delta m \bullet V}{f_k t \bullet A \bullet m} = \frac{\Delta m \bullet d}{f_k t \bullet m} = \frac{\Delta m \bullet d}{F \bullet m} \tag{1}$$

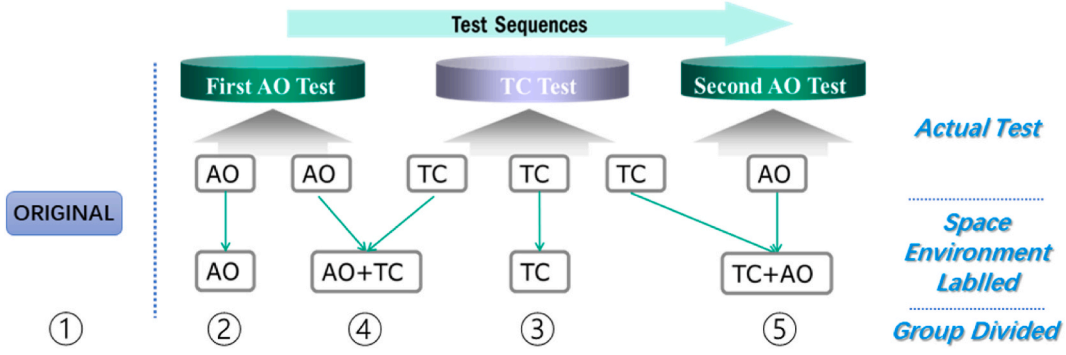

Fig. 2. Layout of the test.

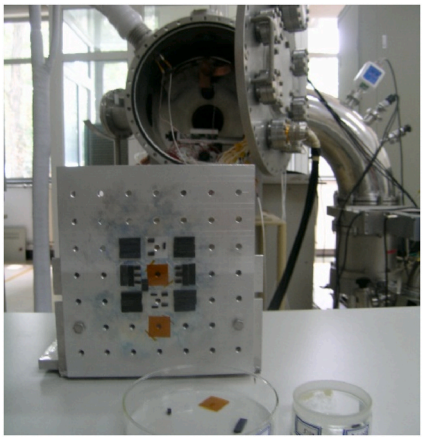

Fig. 3. Layout of the AO test.

where, R_e is the AO interaction rate of the test material，cm^3/atom;

F is AO fluence，atoms/cm^2;

ρ is the density if the specimen, g/cm^3

f_k is AO flux，atoms/cm^2/s.

A is area of exposure，cm^2

t is the duration of the AO test, s

Δm is the mass loss of the specimen，g;

m is the mass of the specimen, g;

d is the thickness of the specimen ，cm

Optical morphology observation was conducted on the OLYMPUS GX-51 optical microscope at BISEE; SEM observation was conducted on the Quanta 200 type Scanning Electron Microscope.

Surface chemical analysis was based on the results from VGDSCALABMKIIX-Ray Photoelectron Spectroscopy.

Inter-laminar shear strength (ILSS) test was conducted follow the GB/T 30969-2014 standard, with loading speed atυ = 1.3 mm/min.

4. Test results and analysis

4.1. Surface Optical Morphology

Optical Morphology was observed before and after the space environment tests, as illustrated in Fig. 4(M40/DFA-1) and Fig. 5 (M40/AG-80). Comparing to the original specimen, Group② (which undergone AO test) has an obvious erosion on the surface, with the carbon fiber exposed(Fig. 4②); while Group③ (which undergone TC test) reveals non-significant denudation in the surface resin, but obviously darkened in color and texture; Specimen undergone (AO + TC) (TC + AO) sequent tests(Group④and Group⑤) are observed too, which reveals no notable difference. Basically, specimen suffered from AO test within, were all had their surface fiber exposed more or less. Whereas, the darkening of the resin may be caused by the recomposing of the functional group, which has different refractive index.

4.2. Surface Microtopography Analysis (by SEM)

Surface Microtopography Analysis was conducted by Scanning Electron Microscope, before and after the space environment test, as illustrated in Fig. 6, Fig. 7.

Common features revealed on the surfaces of both of the materials are:(1) *Carpet*-like surface microtopography could be identified as the remarkable changing after AO test, however, no noticeable feature that worth to be mentioned after TC test; (2) Specimen

Table 1
Atomic oxygen interaction rate under AO and TC + AO test condition.

Material	Atomic Oxygen Reaction Rate ($\times 10^{-24}cm^3$/atom)	
	AO	TC + AO
M40/DFA-1	2.37	2.33
M40/AG-80	4.63	3.95

Table 2
Contrast of the variation of the mass loss rate.

Material	d (AO)	d (TC)	d(AO + TC)	d (TC + AO)	d(AO)+d(TC)
M40/DFA-1	0.33%	0.086%	0.425%	0.193%	0.416%
M40/AG-80	0.41%	0.089%	0.511%	0.325%	0.499%

Table 3
Contrast of the Variation of the specimen's ILSS.

Material	⊿AO	⊿TC	⊿ (AO + TC)	⊿ (TC + AO)	⊿AO+⊿TC
M40/DFA-1	−2.63 MPa	+3.11 MPa	−0.91 MPa	+0.38 MPa	+0.48 MPa
M40/AG-80	−0.90 MPa	+4.54 MPa	−0.06 MPa	+2.36 MPa	+3.64 MPa

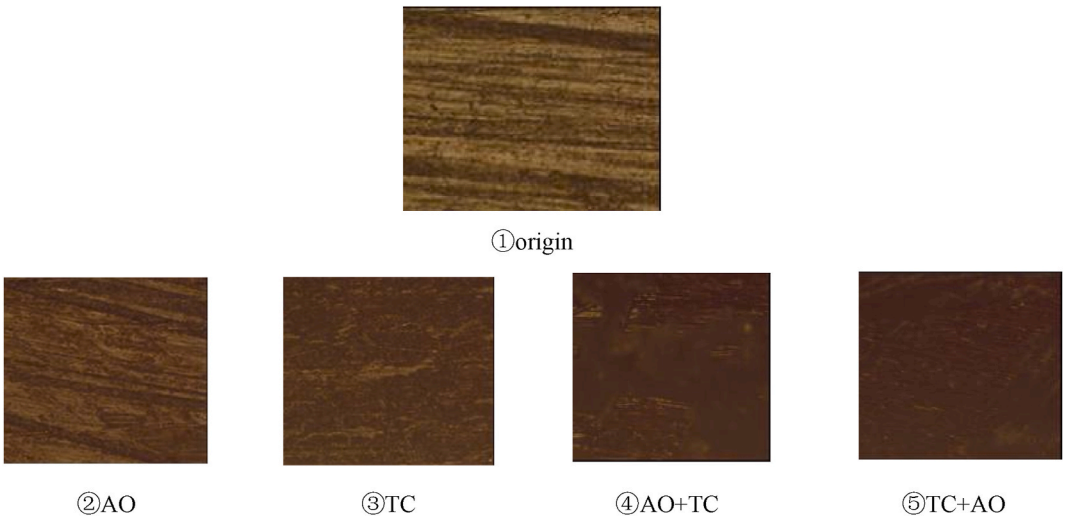

Fig. 4. Surface Optical Morphology of M40/DFA-1.

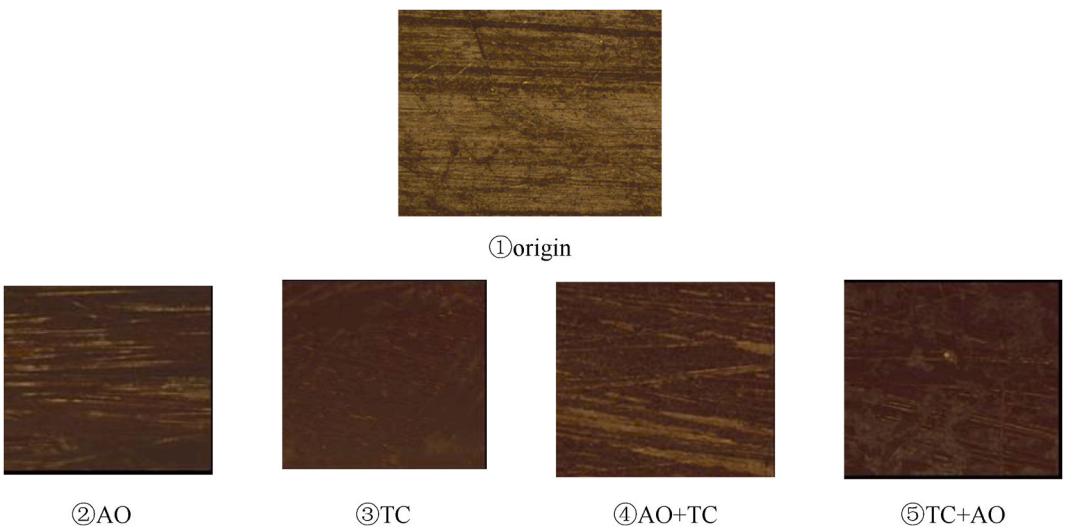

Fig. 5. Surface Optical Morphology of M40/AG-80.

withstood (AO + TC) sequent test demonstrated plenty of carbon fibers exposed near the surface, some of which were ruptured individually; on the other hand, specimen withstood (TC + AO) sequent test had the resin eroded *carpet*-like to some extent, but it was still relatively unapparent comparing to the Group suffered from (AO + TC) test.

4.3. Mechanical performance analysis

4.3.1. Mass loss rate and AO reaction rate

Mass of the specimen were weighed before and after the exposure. The result present a tiny declination on all the group of material. The mass reduction is primarily due to the volatile created by the bond-breaking induced fragments. For example, an O-atom addicted to C atom on the surface followed by H atom elimination, and after that high-energy collisions could either knock weakly bound CO or CO_2 off the surface directly or cause a reaction that would subsequently liberate these molecules [22]. Mass loss and AO reactive rate (those had AO test within) was calculated based on the data collected, and the mass loss was expressed in Fig. 8.

AO reactive rate presented in Table 1 (which is consistent with MISSE 2 In-Space data [38]in rational difference) could manifest directly, that, specimen undergone TC test could enervate the AO interaction with the material, which means, TC experience could enhance the material's resistance to AO erosion-that is in accordance with the phenomenon observed from surface morphology.

The coalescence of the voids (mass loss) means the reduction of the materials -, which would definitely reduce the sample's capability to withstand the stress loads. When the specimens could not withstand the load anymore, they fractured. Coalescence into critical-sized voids could occur at any location along the specimen. Therefore, the observed phenomenon mentioned above should have some correlations with the mechanical strength test.

4.3.2. Inter-laminar shear strength (ILSS) Test

Inter-laminar strength test was conducted before and after space environment test, as illustrated below in Fig. 9.(Detailed data was laid in Table S4 in Appendix).

Some common features could be extracted from the data of ILSS for both materials that: (1) ILSS performance (which verified the prediction) declined after AO test, whereas it inclined after TC test; (2) Both AO single test and (AO + TC) sequent test weaken the materials' ILSS, of which, the sequent test has a relatively lower amplitude; (3) Both TC single test and (TC + AO) sequent test enhanced the material's ILSS, of which, the latter is relatively less conspicuous.

4.4. X-Ray photoelectron spectroscopy analysis

4.4.1. M40/DFA-1

C1s peak spectrum from the XPS of the M40/DFA-1 materials was demonstrated in the following Fig. 10. Basically, the superposition of components of typical functional groups in which the atom is involved, shapes the peaks—based on the acknowledgement that photoelectrons binding energy is influenced by the electron density [20]. Peak decomposition could elucidate the chemical nature of the organic compounds., The components of the C1s peak were as follows:285eV, always refers to carbon only bound to carbon and hydrogen[**C**-(C,H)]; 286.5eV, attributed to carbon making a single bond with oxygen or nitrogen[**C**-(O,N)]; 288.6 eV, assigned to carbon making a double bond with oxygen as in amide function [C-(**C**═O)–N]; near 289.0eV, assigned to carbonyl or ester functions [C-(**C**═O)–O],respectively [20].

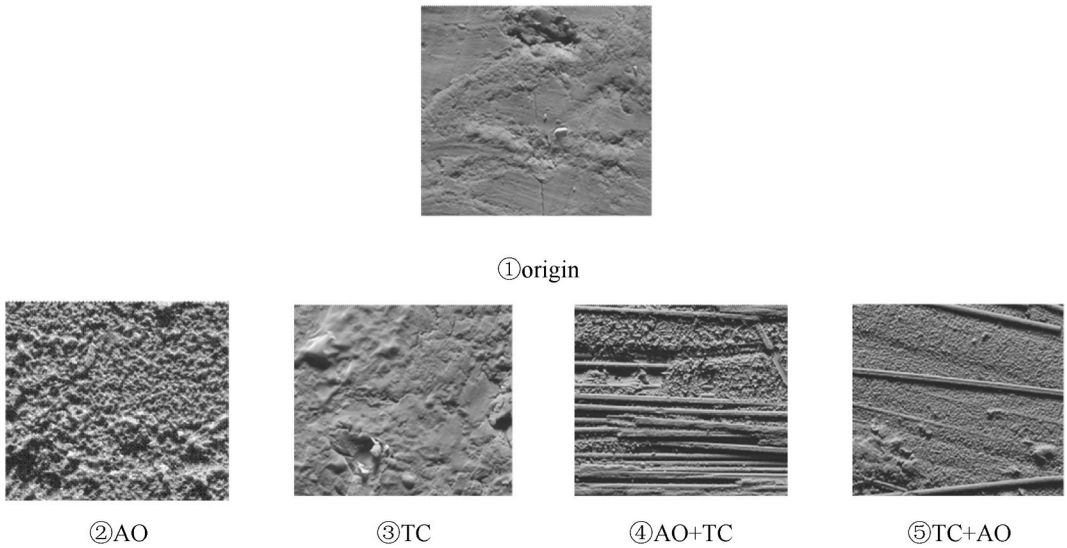

Fig. 6. Surface Microtopography of M40/DFA-1.

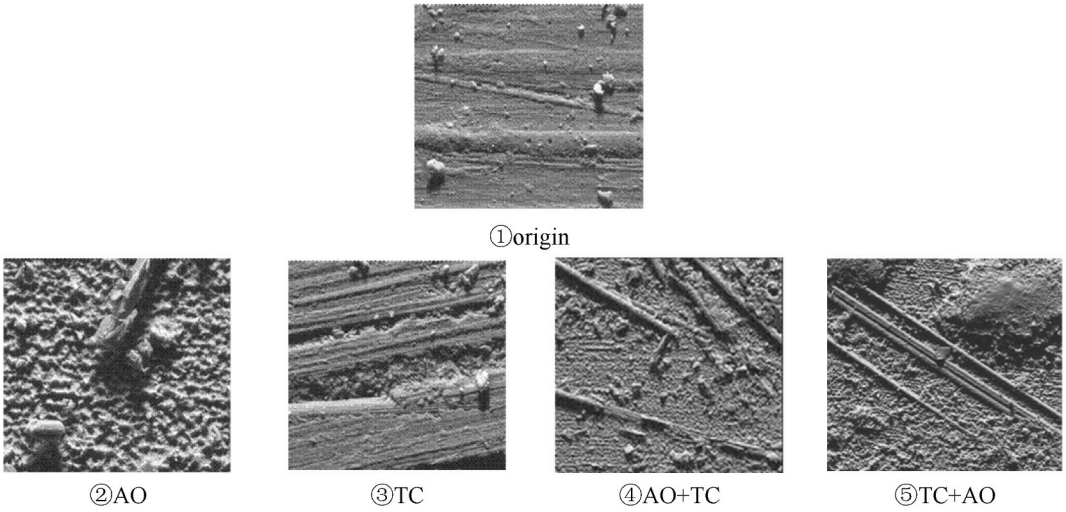

Fig. 7. Surface Microtopography of M40/AG-80.

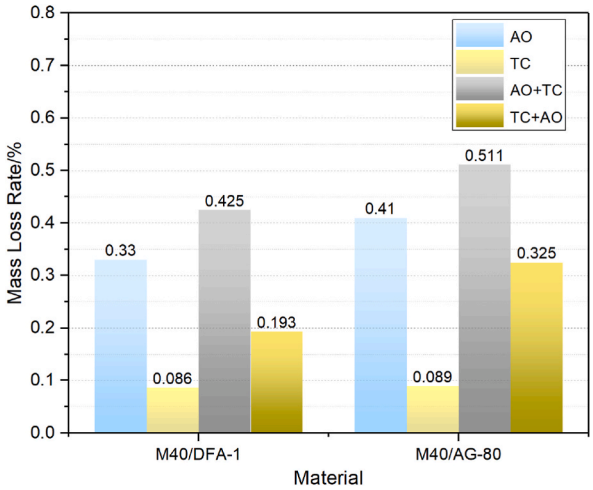

Fig. 8. Mass loss rate of specimen under different test condition.

Spectrum of original specimen is represented in Fig. 10①. However, C1s spectrum, representing specimen undergone AO environment at 1.5×10^{20}atoms/cm^2, had got some difference, as illustrated in Fig. 10②. After the AO exposure, intensity of C_a peak(C–C bond) located at 285eV dropped drastically，from 70.20% to 21.78%; while C_b peak(C–*O*–C bond)located at 286.5eV escalated from 27.82% to 58.37%; besides, C_c peak(C═O bond)located at 289eV had also got a rise, from 6.66% to 19.85%. That is because the O atoms de-bonded the C–C bonds and generated C–O • bonds, and then, reformed C–*O*–C bonds with the adjacent C afterwards [39], hence the intensity of the peak at 286.5eV raised. - -Due to the 3.60 eV bonding energy, C–C bond was broken primarily; and then the other two C–H bond(4.28 eV) linked with the C atom in the C–O bond also be oxidized out to form a C═O bond [39]—that is the reason why the intensity raised as well. The more C–*O*–C generates, the greater the crosslinking declined. That would enhance the toughness, but weaken the strength, which is consistent with the result of ILSS. Fig. 10③ demonstrated the C1s peaks from the specimen undergone TC test. Comparing to the specimen stay in the original state, the three peaks of C_a，C_b，C_c all moved towards the lower binding energy. Besides, intensity of C_a peak (C–C bond) increased from 70.20% to 77.29%, while that of C_b peak (C–*O*–C bond) decreased from 27.82% to 14.22%. That indicates, more C–C bonded directly after TC test—that would raise the resin matrix crosslinking density, hence, strengthen the mechanical performance—the ILSS test revealed the coherent result. In addition, TC test had brought about the relocation of the peak position, that indicates, the circumstances C atoms settled in had changed, newly-generated substances might come into form.

C1s peak spectrum analysis of M40/DFA-1 undergone AO + TC and TC + AO was illustrated in Fig. 10④⑤ respectively. Comparing the two different sequent tests, C_a peak intensity of the former is 34.83%，which is obviously lower than the latter (of which is 69.8%); C_b peak intensity of the former is 55.80%，which is higher than the latter(of which is 19.58%); besides, that of the C_c peak is

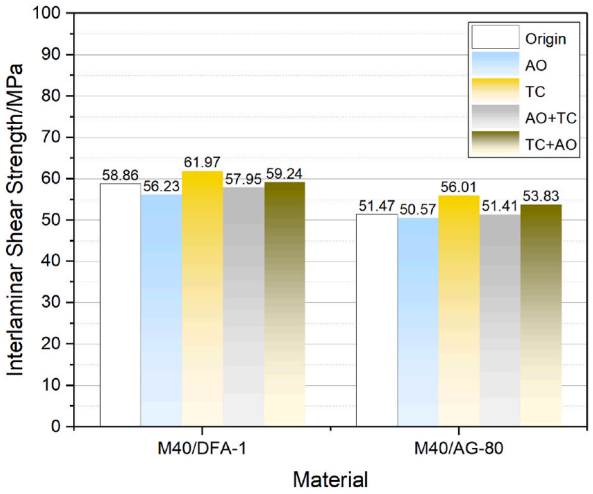

Fig. 9. Contrast of the ILSS of specimen.

almost equal. Information stated above indicated that (AO + TC) sequent test facilitate more C–C bonds reformed into C–*O*–C bond. O atom inserted into C–C bond would form into C–*O*–C bond—so that rarefied the resin matrix crosslinking density, further declined the mechanical strength—which is consistent with the result of ILSS performance.

4.4.2. M40/AG-80

C1s peak spectrum from the XPS result of the M40/AG-80 material was demonstrated in the following Fig. 11.

As illustrated in Fig. 11①，peak spectrum of M40/AG-80 involved with three peaks as well. Before space environment test, C_a peak (C–C bond on the Benzene ring) takes the percentage of 35.62%, C_b peak(C–*O*–C bond) takes the percentage of 45.9%, while C_c peak(C═O bond) takes intensity of 35.52%. As illustrated in Fig. 11②, specimen undergone AO environment were analyzed. Intensity of C_a peak(C–C bond) and C_b peak(C–*O*–C bond) were both declined, while intensity of C_c peak(C═O) escalated conspicuously. It implies that plenty of C–C bonds(3.60eV) and C–O bonds(4.28eV) de-bonded and reformed into C═O bonds. Fig. 11③ demonstrated M40/AG-80 material's spectrum after TC test. The peak position switch towards the low-energy side, it implies some newly-generated substances had appeared.

In addition, intensities of C_a peak and C_c peak were both heightened while C_b peak dropped. That indicates, C–*O*–C bond were consumed into C–C bond, and reformed into C═O bonds, this type of combination could strengthen the crosslinking density, further promote the ILSS performance—it could be validated by the test result correspondingly.

Fig. 11④⑤ demonstrated C1s spectrum of the M40/AG-80 material undergone AO + TC and TC + AO sequent tests. C_a peak intensity declined in the former sequent, whereas, it inclined in the latter sequent; It seems almost equal for the C_b peak; C_c peak had a dramatical rise in the former sequent while it dropped noticeable in the latter sequent. Information stated above indicates that C–C in the former sequence were oxidized more severely, which established relatively more C═O bond; on the other hand, C–C bond was preserved relatively more (with less C═O formed) in the latter sequence—which indicates that TC has enhanced the specimen's resistance to the AO interaction—therefore, raise the crosslinking density, further, lead to a better mechanical performance. This interpretation could be confirmed in the corresponding ILSS test.

5. Synergistic effects analysis and discussion

5.1. Mass loss rate

The mass loss rate focusing on the summation of the both environment factors was sorted into Table 2, from the piles of data from space environment tests (laid in Table S2, Table S3 in the Appendix) .

Contrast among the posterior three columns could dig out the following simple common trait，which is:

$$d(\mathrm{AO}+\mathrm{TC}) > \mathrm{d}(\mathrm{AO}) + \mathrm{d}(\mathrm{TC}) > \mathrm{d}(\mathrm{TC}+\mathrm{AO}) > 0$$

Number Axis was employed in the comparison of the values, as demonstrated in Fig. 12：

For the material of M40/DFA-1，$\frac{d(AO+TC)}{d(AO)+d(TC)} = \frac{0.425\%}{0.33\%+0.086\%} = 1.0216$，$\frac{d(TC+AO)}{d(AO)+d(TC)} = \frac{0.193\%}{0.33\%+0.086\%} = 0.4639$.

For the material of M40/AG-80，$\frac{d(AO+TC)}{d(AO)+d(TC)} = \frac{0.511\%}{0.41\%+0.089\%} = 1.0240$，$\frac{d(TC+AO)}{d(AO)+d(TC)} = \frac{0.325\%}{0.41\%+0.089\%} = 0.6513$.

Therefore, both materials correspond to the commonality as $\frac{d(AO+TC)}{d(AO)+d(TC)} > 1$ and $1 > \frac{d(TC+AO)}{d(AO)+d(TC)} > 0$，which implied that the combined effects of AO and TC are not simple summation, further, different sequence would lead to different combined effects—even optimized or deteriorated are not that easy for sure.

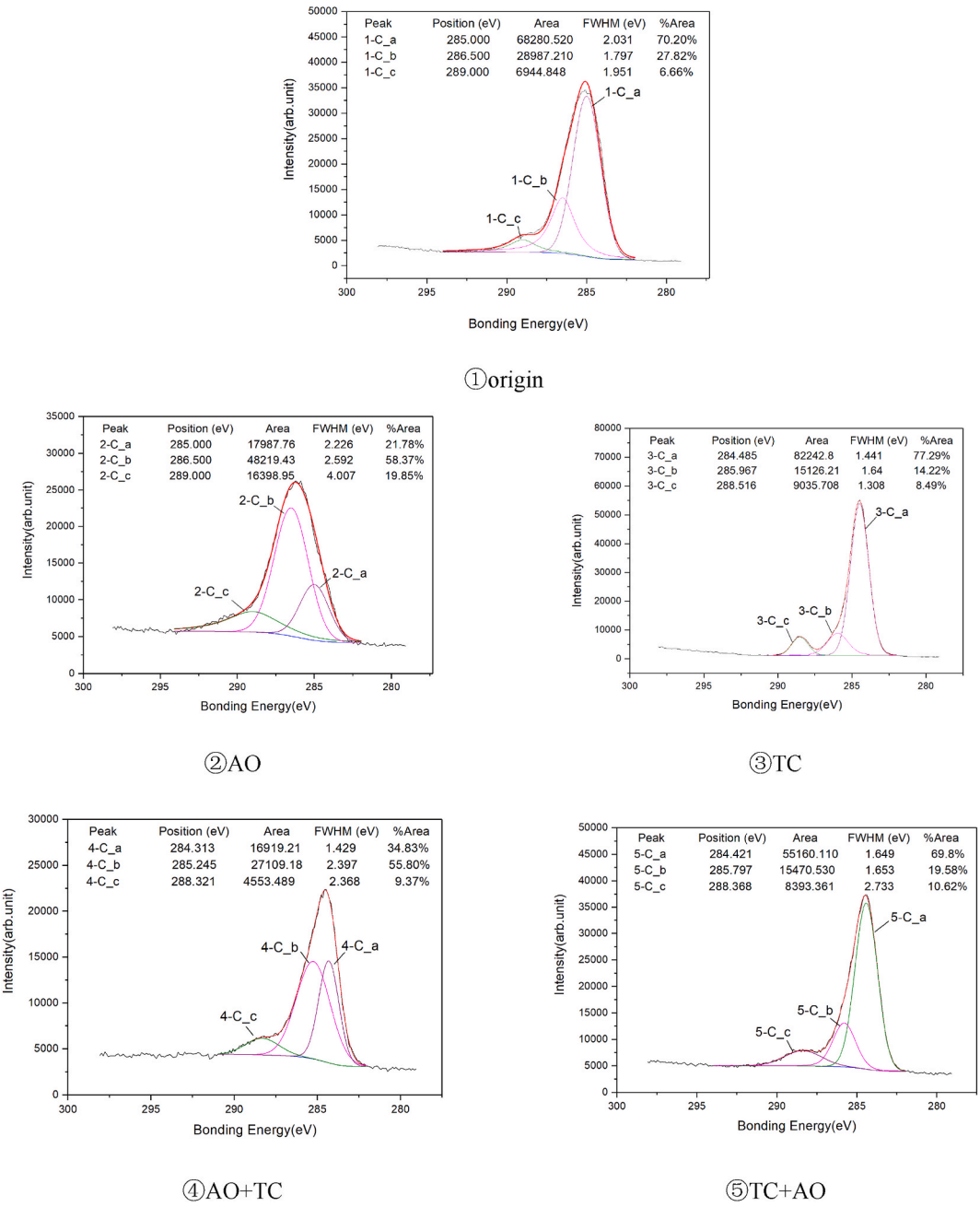

Fig. 10. X-Ray photoelectron spectroscopy of M40/DFA-1.

5.2. Inter-laminar shear strength (ILSS)

Focusing on the summation characteristic of the AO and TC effects on the ILSS performance , data could be sorted as in the following Table 3.

The posterior three columns were identified and illustrated as Fig. 13 and Fig. 14, and the common features were circled out by the dotted lines.

Based on the information given above, commonality could be extracted and deduced, as follows:

$\Delta AO < 0$, $\Delta TC > 0$;and $\Delta AO + \Delta TC > \Delta(TC + AO) > 0 > \Delta(AO + TC)$.

We could interpret the information respectively, and have an attempt to push forward to a logical comprehension:

(1) $\Delta AO < 0$, $\Delta TC > 0$; $\Delta AO + \Delta TC > 0$.

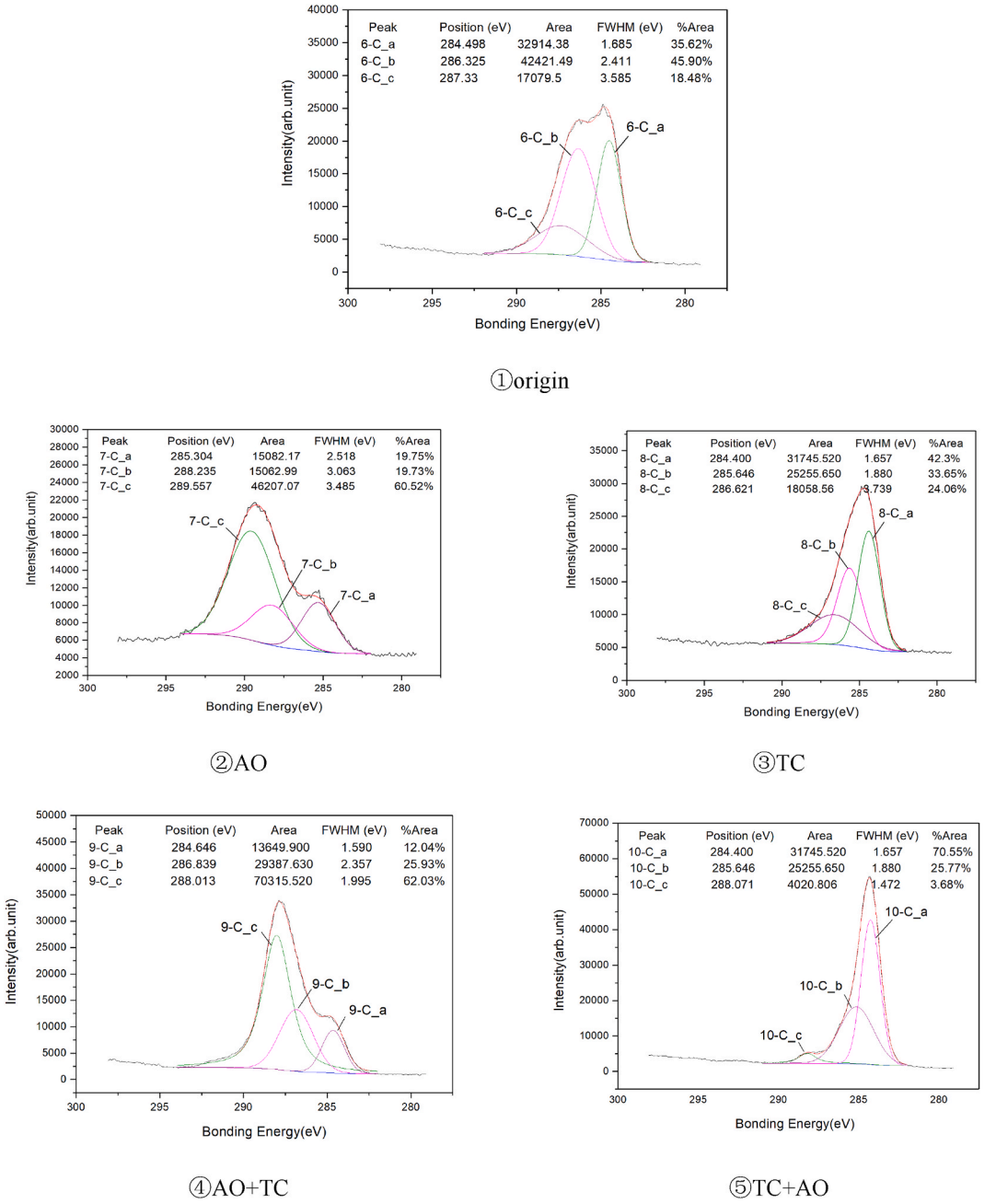

Fig. 11. X-Ray photoelectron spectroscopy of M40/AG-80.

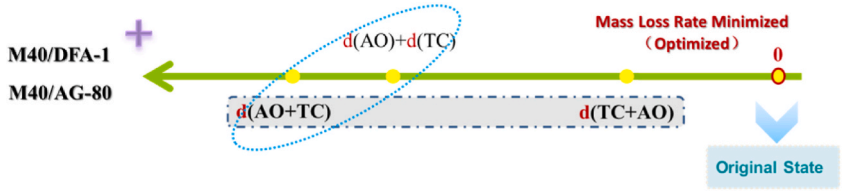

Fig. 12. Contrast of the Mass Loss of the two materials.

Under the condition in this study, the effects of AO interaction on the materials' ILSS seems negative(lower the ILSS strength)，while TC led to a positive effect(raise the ILSS strength); besides, the amplitude TC optimized is greater than that AO degraded.

(2) $\Delta TC + \Delta AO > 0 > \Delta(AO + TC)$ (Marked in the sky-blue dotted circle)

Firstly，$\Delta(AO+TC) \neq \Delta AO + \Delta TC$ implies that (AO + TC) sequent test effect is not equivalent to the simply summation of each. Secondly，$\Delta(AO+TC) < 0$ implies that, specimen gone through the AO test, had an rise on the ILSS performance when undergoing the subsequent TC test at an amplitude weaker than the harm AO brought-therefore,(AO + TC) sequent test result in a degradation in the ILSS performance in the end. Last but not least, if we put $\Delta(AO+TC) < 0$ with $\Delta AO + \Delta TC > 0$ together, we could further deduce that，specimen pre-tested with AO environment, would perform an obviously tiny raise in ILSS when undergoing the subsequent TC test. That might be because of the change in the molecule structure in the surface resin matrix due to the AO interaction—on one hand, result in the lower rise in the molecule crosslinking under TC environment test; on the other hand, the mass loss of volatile(CO、CO_2、NO_2)increased under TC test, which would decrease the ILSS.

Generally speaking，AO interaction could affect the subsequent TC effect to the material; (AO + TC) sequent test is more severe to the summation of AO/TC single factor effects.

(3) $\Delta AO + \Delta TC > \Delta(TC + AO) > 0$ (Marked in the orange dotted oval)

Firstly，$\Delta(TC+AO) \neq \Delta AO + \Delta TC$ implies (TC +AO) sequent test effect is not equivalent to the simple summation either. Secondly, $\Delta(TC+AO) > 0$ indicates that, specimen undergone TC test, would result in a declination in ILSS after suffering from the AO test, but to an amplitude weaker than that TC enhanced, hence lead to an increasement in the ILSS performance after the whole (TC+ AO) sequent test. Further，$\Delta(TC + AO) < \Delta AO + \Delta TC$, which implies specimen undergone TC test firstly would suffer a more severe degradation in ILSS under subsequent AO test(compare to the specimen interaction with AO directly)，it means, TC amplified the damage that AO brought. But worth to be mentioned that, the comparison of mass loss and AO interaction rate indicates that, TC test could desensitize the AO interaction rate. That could be explicated as that TC environment would change the molecule chain structure through post-curing process, although the newly-generated structure has got a reduction in mass loss in the process of AO test, but has also got a relatively weaker structure in the AO interaction (compare to the specimen that interact with AO environment directly)—that is correspond to the displacement of the peak position observed in the XPS analysis.

Generally speaking, TC environment pre-testing would affect the subsequent AO interaction with the material, (TC + AO) sequent test would bring a relatively weaker rise comparing to the simple summation of AO/TC single factor effects.

(4) $\Delta(TC + AO) > 0 > \Delta(AO + TC)$ (Marked as dotted square frame filled with grey)

It could be explicated as that, whether the environment test would optimize the ILSS or deteriorate it, that should be pending. Data from this work unravels that, sequent test with TC conducted first would enhance the ILSS performance, whereas, AO conducted first would weaken it.

5.3. *Discussion of AO&TC synergistic effects*

Firstly, either for the mechanical performance or the mass loss, (AO + TC) sequent test would bring the most harsh damage to the material, which is more severe than both AO/TC single test effect and (TC + AO) sequent test.

Secondly, (TC + AO) sequent test result in the minimum mass loss，which could be further deduced that TC could strengthen the resistance to AO erosion.

Thirdly, on the contrary to the clauses mentioned above, (TC + AO) sequent test haven't got the most optimized ILSS, though. That could be interpreted as that materials endured TC environment would be more tending to have C–C in the core chain de-bonded and oxidized, which yielded volatile gases, when they encountered with AO afterwards. Therefore, do more damage to the mechanical performance, but, with a relatively minor mass loss.

At the meantime, it could be manifested that, two manners exists in the process TC influencing materials: on one hand, atoms and tiny functional group near the surface or besides the voids would release volatile gases—that would lead to the mass loss(whether due to physical or chemical evolution); on the other hand, volatile yield from the material were more likely formed from those atoms and

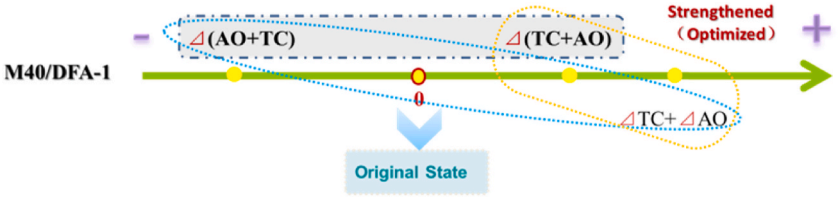

Fig. 13. Contrast of the ILSS variation of M40/DFA-1.

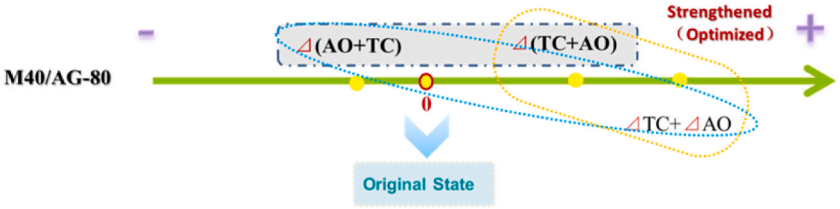

Fig. 14. Contrast of the ILSS variation of M40/AG-80.

functional group which are located on the non-core chain or between two C atoms(which is self-consistent with result from XPS), therefore, the process of de-bonding and oxidation would reinforce the ILSS along with mass loss reversely.

Last but not the least, limited to the capability of ground-based test facilities, AO&TC synergistic effects test could hardly be conducted simultaneously till now. However, if we nominate both (AO + TC) and (TC + AO) as *sequent test* uniformly. Then, based on the result of the sequent test, synergistic effects do exist between AO and TC space environment. Besides, comparing result from *sequent test* to the result from summation of AO/TC single factors , both materials revealed that, *ILSS* from *sequent test* would be weaker than the simple summation of factors' effects.

If we consider, AO/TC test conducted simultaneously, as a series of infinite tempo time-zones (AO + TC)+(TC + AO)+(AO + TC)+ … …summing up in an infinite cycle as expressed in Equation (2), then, synergistic effects of the two factors should be between Δ(AO +TC) and Δ(TC + AO).Further, we could conclude that the degradation after AO&TC synergistical conduction would be more severe than the simple summation of single factors' effects.

$$\Delta(AO\&TC) \approx d(AO+TC) + d(TC+AO) + d(AO+TC) + \cdots\cdots \tag{2}$$

That is to say, it is insufficient to employ simple summation of single factors' effects to represent the integral effects result in the practical orbiting when referring to the AO and TC environment. In a word, there seems kind of deficiency in the environment test.

6. Nomination of Summation Co-efficiency [40]

Focusing on the materials selected in this research, we could conclude that synergistic effects do exist between AO and TC environment, basically.

Further, for the purpose to decide that, to which extent that the synergistic effects correlating– an index K nominated as *Summation Co-efficiency*, might be put forward to characterize this consideration of quantified evaluation criteria. We define K by Equation (3) as following:

$$K = \frac{K_{(AO+TC)} + K_{(TC+AO)}}{2} \tag{3}$$

where,

$K_{(AO+TC)} = \frac{\Delta(AO+TC)}{\Delta AO+\Delta TC}$, $K_{(TC+AO)} = \frac{\Delta(TC+AO)}{\Delta AO+\Delta TC}$.If $K \neq 1$, that indicates there's some correlation in the process of two factors interacting with material, we comprehend it as synergistic effects; while $K = 1$ is comprehended as nothing correlated between the two factors interaction with material. Further more, we nominate an supplementary index K_0 as an more perceptual indicator, defined as Equation (4):

$$K_0 = \left| \frac{K_{(AO+TC)} + K_{(TC+AO)}}{2} - 1 \right| \tag{4}$$

The major K_0 is, the greater correlation in between.

We define K_M as *Summation Co-efficiency of Mass Loss* , K_S as *Summation Co-efficiency of Inter-laminar Shear Strength*, then, synergistic summation characteristics of the mass loss and ILSS of the two materials could be calculated based on the data from test, as laid in Table 4.

K_M and K_S of M40/DFA-1 are both higher than that of M40/AG-80, thus, we deem the synergistic sensitivity of M40/DFA-1 is higher than that of M40/AG-80.

Table 4
Summation Co-efficiency of the tested specimen.

Material	K_M	K_S
M40/DFA-1	0.26	1.55
M40/AG-80	0.16	0.68

7. Conclusion

Based on the matrix-patterned ground-based test, assisted by the analyzation expounded above, several conclusions could be summarized in below:

(1) *Aspect of the space environment effects*: Synergistic effects do exist in AO&TC environment. Under the circumstances that excluded microcracks appearance, TC would enhance the resistance of the resin-matrixed composite materials; Synergistic effects referring to the mechanical characteristics would between the results of the two different sequent tests, therefore, logically speaking, it should be weaker than the simple summation of the AO/TC single factors' effects.
(2) *Aspect of test method*: (AO + TC) sequent test is more rigorous comparatively either from the prospect of the surface morphology, mass loss or mechanical performance, nevertheless, it might lead to over-testing as a result.
(3) *Aspect of material evaluation*: Synergistic effects between AO&TC reflected on the material of M40/DFA-1 is revealing to be more sensitive than that of M40/AG-80.
(4) *Aspect of mechanism discussion*: Through the surface components analysis, comparatively more C–C bond were preserved or regenerated under the (TC + AO) sequent test, which would reserve a relatively higher crosslinking density—that give rise to a more higher strength—it could be confirmed in the corresponding ILSS tests.
(5) *Aspect of synergistic characterization:* A quantified criterion K nominated to characterize the synergistic correlation could be employed, so as to expand the dimension for material selection and space environment evaluation. Furtherly, it might be possible to give a little push to the data accumulation and exploration for some future potentials.

In general, some primary advices could be given for spacecraft design and testing, such that, in the aspect of spacecraft design, materials with K at lower value should be better to be selected, to reduce the risks under the circumstances that synergistic effects almost leads to aggravation(that is to say that the index K could act as an additional characteristic to describe a space material and serve for material selection like the NASA's MAPTIS [37]does; while, in the aspect of testing design, sequent test is necessary （simultaneous testing is better after the facilities has been established), and it would be better to choose the AO→TC method, which is more severe to challenge the material performance before application, thus ，to consolidate the reliability of the space activities.

The data could be retrieved from the appendix and reproduced through the test.

Declaration of competing interest

The authors declare that they have no known competing financial interests or personal relationships that could have appeared to influence the work reported in this paper

Appendix A. Supplementary data

Supplementary data to this article can be found online at https://doi.org/10.1016/j.heliyon.2023.e17431.

References

[1] Xiaoning Yang, Yong Yang, Space Environment Engineering for Spacecraft, Beijing Institute of Technology Press, Beijing, 2018, pp. 24–243.
[2] S. Calders, N. Messios, E. Botek, E. De Donder, M. Kruglanski, Modeling the Space Environment and its Effects on Spacecraft and Astronauts Using SPENVIS. 2018 SpaceOps Conference, AIAA, Marseille, France, 2018, pp. 2018–2598.
[3] Susan W. Samwel, Esraa A. El-Aziz, B. Henry, B. Garrett, Ahmed A. Hady, Makram Ibrahim, Magdy Y. Amin, Space radiation impact on smallsats during maximum and minimum solar activity, Adv. Space Res. 64 (2019) 239–251.
[4] Yanjun He, AlexBrinkmeyer AgnieszkaSuliga, IanHamerton MarkSchenka, Atomic oxygen degradation mechanisms of epoxy composites for space applications, Polym. Degrad. Stabil. 166 (2019) 108–120.
[5] G. RivalabT, PaulmieraE. Dantrasb, Influence of electronic irradiations on the chemical and structural properties of PEEK for space applications, Polym. Degrad. Stabil. 168 (2019), 108943.
[6] Sharon, K.R. Miller, Bruce Banks. Degradation of spacecraft materials in the space environment, MRS Bull. 35 (2010) 20–24.
[7] R. Pastore, A. Delfini, M. Albano, A. Vricella, M. Marchetti, F. Santoni, F. Piergentili, Outgassing effect in polymeric composites exposed to space environment thermal-vacuum conditions, Acta Astronaut. 170 (2020) 466–471.
[8] Yun Cui, Zicai Shen, Jiawen Qiu, Wei Dai, Yuanan Zhao, Jianda Shao, Effects of space environments on optical component molecular contamination and their mitigation methods, Spacecraft Environ. Eng. 39 (6) (2022) 651–660.
[9] Qi Ouyang, Wenwen Wang, Qiang Fu, Dongmei Dong, Atomic oxygen irradiation resistance of transparent conductive oxide thin films, Thin Solid Films 623 (2017) 31–39.
[10] Verker Ronen, Eitan Grossman, Irina Gouzman, A novel method for on-orbit measurement of space materials degradation, Rev. Sci. Instrum. 82 (2011), 023901.
[11] Eiji Miyazaki, Masahito Tagawa, Kumiko Yokota, Rikio Yokota, Yugo Kimoto, Junichiro Ishizawa, Investigation into tolerance of polysiloxane-block-polyimide film against atomic oxygen, Acta Astronaut. 66 (2010) 922–928.
[12] Wen Zhang, Min Yi, Zhigang Shen, Xiaohu Zhao, Xiaojing Zhang, Shulin Ma, Graphene-reinforced epoxy resin with enhanced atomic oxygen erosion resistance, J. Mater. Sci. 48 (2013) 2416–2423.
[13] Yun Cheng, Xiaoqian Chen, Tao Sheng, In situ measure of atomic oxygen flux using a silver film sensor onboar "TianTuo 1" nanosatellite, Adv. Space Res. 57 (2016) 281–288.
[14] K.R. Miller Sharon, Atomic Oxygen Effects, NASA Glenn Research Center, GRC-E-DAA-TN16377, 2015, p. 13.

[15] Jing Zhang, Ling Ai, Li Xiao, Xianpeng Zhang, Yuehui Lu, Guofei Chen, Xingzhong Fang, Ning Dai, Runqin Tan, Weijie Song, Hollow silica nanosphere/polyimide composite films for enhanced transparency and atomic oxygen resistance, Mater. Chem. Phys. 222 (2019) 384–390.
[16] Liam S. Morrissey, Rahnamoun Ali, Nakhla Sam, The effect of atomic oxygen flux and impact energy on the damage of spacecraft metals, Adv. Space Res. 66 (2020) 1495–1506.
[17] A. Delfini, F. Santoni, F. Bisegna, F. Piergentili, R. Pastore, A. Vricella, M. Albano, G. Familiari, E. Battaglione, R. Matassa, M. Marchetti, Evaluation of atomic oxygen effects on nano-coated carbon-carbon structures for re-entry applications, Acta Astronaut. 161 (2019) 276–282.
[18] Naoki Shimosako, Yukihiro Hara, Kazunori Shimazaki, Eiji Miyazaki, Hiroshi Sakama, Effects of atomic oxygen on titanium dioxide thin film, Acta Astronaut. 146 (2018) 1–6.
[19] Timothy K. Minton, Michael E. Wright, Sandra J. Tomczak, Sara A. Marquez, Linhan Shen, Amy L. Brunsvold, Russell Cooper, Jianming Zhang, Vandana Vij, Andrew J. Guenthner, J. Brian, Petteys, Atomic oxygen effects on POSS polyimides in low earth orbit, ACS Appl. Mater. Interfaces 4 (2012) 492–502.
[20] Jessem Landoulsi, J. Michel, Genet, Sandrine Fleith, Yetioman toure, Irma Liascukiene, Christophe Methivier, Paul G. Rouxhet. Organic adlayer on inorganic materials: XPS analysis selectivity to cope with adventitious contamination, Appl. Surf. Sci. 383 (2016) 71–83.
[21] Mathew Celina, ErikLinde, Brunson Douglas, Quintana Adam, Nicholas Giron, Overview of accelerated aging and polymer degradation kinetics for combined radiation-thermal environments, Polym. Degrad. Stabil. 166 (2019) 353–378.
[22] Masahito Tagawa, Timothy K. Minton, Mechanistic studies of atomic oxygen reactions with polymers and combined effects with vacuum ultraviolet light, MRS Bull. 35 (2010) 35–40.
[23] Masahito Tagawa, Kumiko Yokota, Atomic oxygen-induced polymer degradation phenomena in simulation LEO space environments: how do polymers react in a complicated space environment, Acta Astronaut. 62 (2008) 203–211.
[24] Lipika Ghosh, Mohammad Harris Fadhilah, Hiroshi Kinoshita, Nobuo Ohmae, Synergistic effect of hyperthermal atomic oxygen beam and vacuum ultraviolet radiation exposures on the mechanical degradation of high-modulus aramid fivers, Polymer 47 (2006) 6836–6842.
[25] Joyce A. Dever, Eric J. Bruckner, Elvin Rodriguez, Synergistic effects of ultraviolet radiation, thermal cycling and atomic oxygen on altered and coated Kapton surface, in: 30th Aerospace Sciences Meeting & Exibit, 1992. AIAA-92-794.
[26] M.M. Mikhailov, A.N. Sokolovskiy, S.A. Yuryev, V.V. Karanskiy, Synergistic effects in the change in optical properties of ZnO powder modified with SiO2 nanoparticles upon sequential irradiation with electrons and solar quanta, Adv. Space Res. 66 (2020) 2703–2710.
[27] BumMoon FirasAwajaaJin, MichaelGilbertdeChun ShengnanZhang, J. GonKimbPaul, Pigramde. Surface molecular degradation of 3D glass polymer composite under low earth orbit simulated space environment, Polym. Degrad. Stabil. 95 (2010) 987–996.
[28] Rong Sui, Wenbo Zhang, Jiang Wei.Experimental study on synergistic effect of atomic oxygen and ultraviolate irradiation on mechanical properties of nylon materials, Spacecraft Environ. Eng. 38 (2) (2021) 171–175.
[29] H.E. Misak, V. Sabelkin, S. Mall, P.E. Kladities, Thermal fatigue and hypothermal atomic oxygen exposure behavior of carbon nanotube wire, Carbon 57 (2013) 42–49.
[30] Davide Micheli, Carmelo Apollo, Roberto Pastore, Ramon Bueno Morles, Plinio Coluzzi, Mario Marchetti, Temperature, atomic oxygen and outgassing effects on dielectric parameters and electrical properties of nanostructured composite carbon-based materials, Acta Astronaut. 76 (2012) 127–135.
[31] H.E. Misak, S. Mall, Characterization of carbon nanotube yarn after exposure to hyperthermal atomic oxygen and thermal fatigue, Adv. Space Res. 58 (2016) 2385–2392.
[32] Roberto Pastore, Andrea Delfini, Fabio Santoni, Mario Marchetti, Marta Albano, Fabrizio Piergentili, Roberto Matassa, Space environment exposure effects on ceramic coating for thermal protection Systems, J. Spacecraft Rockets 58 (2021) 1387–1393.
[33] Stephen S. Tompkins, Effects of thermal cycling on mechanical properties of graphite polyimide, J. Spacecraft Rockets 21 (1984) 274–280.
[34] Sang-Guk Kang, Dong-Hoon Kang, Chun-Gon Kim, Real-time monitoring of transverse thermal strain of carbon fiber reinforced composites under long-term space environment using fiber optic sensors, NDT&E International 42 (2009) 361–368.
[35] Baifeng Yang, Zhufeng Yue, Xiaoliang Geng, Peiyan Wang, Jian Gan, Baohua Liao, Effects of space environment temperature on the mechanical properties of carbon fiber/bismaleimide composites laminates, Proc. Inst. Mech. Eng.: Journal of Aerospace Engineering, Part G 232 (2018) 3–16 (London).
[36] C. Mathew, Celina. Review of polymer oxidation and its relationship with materials performance and lifetime prediction, Polym. Degrad. Stabil. 98 (2013) 2419–2429.
[37] Standard Practices for Ground Laboratory Atomic Oxygen Interaction Evaluation of Materials for Space Applications, ASTM Standard, 2006. E2089-00.
[38] K. Kim, de Groh, Materials International space station experiment (MISSE): overview, NASA glenn's experiments and future needs, NASA:GRE-E-DAA-TN30598 21 (2016) 27.
[39] Jeffrey T. Paci, Hari P. Upadhyaya, Jianming Zhang, George C. Schatz, Timothy K. Minton, Theoretical and experimental studies of the reactions between hyperthermal O(3P) and graphite: graphene-based direct dynamics and beam-surface scattering, J. Phys. Chem. A 113 (2009) 4677–4685.
[40] RQ.Zhai, et al., Faming Zhuanli Shenqing Gongkai Shuomingshu, ZL201910375011.0.